International Conference on Mathematics, Computational Methods & Reactor Physics (M&C 2009)
Saratoga Springs, New York, May 3-7, 2009, on CD-ROM, American Nuclear Society, LaGrange Park, IL (2009)

AN ALTERNATIVE STOCHASTIC DOPPLER BROADENING ALGORITHM

B. Becker, R. Dagan, C.H.M. Broeders
Institute for Neutron Physics and Reactor Technology (INR)
Forschungszentrum Karlsruhe GmbH
Postfach 3640, D-76021 Karlsruhe, Germany
becker@inr.fzk.de; dagan@inr.fzk.de; broeders@inr.fzk.de

G. Lohnert
Institute of Nuclear Technology and Energy Systems (IKE)
University of Stuttgart
Pfaffenwaldring 31, D-70569 Stuttgart, Germany
lohnert@ike.uni-stuttgart.de

ABSTRACT

The temperature dependent, ideal gas scattering kernel for heavy nuclei with pronounced resonances was developed, proved and implemented in the data processing code NJOY from which the scattering probability tables were prepared. Those tables were introduced to the well known MCNP code. The analytic solution of this scattering kernel is consistent with the Doppler Broadening method of D. E. Cullen and C. R. Weisbin.
In this study we present an alternative stochastic algorithm based on MCNP subroutines which allows for Doppler broadening of the integral as well as double differential cross section. The analytical solution of the kernel is confirmed. This stochastic method is then introduced into the MCNP code by means of a rejection method, suggested originally by W. Rothenstein. The differences between the new kernel and the standard MCNP kernel are illustrated for specific resonances of U238, Th232, Au197 and Hg199.
LWR unit cell calculations are performed and criticality, reaction rates and Doppler reactivity coefficients are calculated. Based on comparison with the analytical (probability S(α,β)-tables) approach it is confirmed that the stochastic algorithm gives accurate results. The differences lie within 1-2 standard deviations for all practical cases that were analyzed.

Key Words: Scattering Kernel, Doppler Broadening, DBRC

1. INTRODUCTION

The well known Doppler Broadening Algorithm which is integrated within the Data Processing code NJOY [8] is based on the SIGMA1 code developed by Cullen and Weisbin [9]. The resulting Doppler broadened integral cross sections are then introduced in neutron-physics codes and in particular in the stochastic transport codes like MCNP [7]. Contrarily the differential part of the scattering cross section is usually approximated at 0 K. The first expression of a temperature dependent scattering kernel was developed by E. Wigner and J. Wilkins [1]. Their isotropic kernel introduced the energy transfer from a neutron to a target nucleus without internal structures. Their publication was followed by a lot of studies, some of which dealing also with isotopes with energy dependent cross sections [2, 3, 4]. In 1998 Rothenstein and Dagan [5]

extended those studies and presented the full double differential, temperature dependent scattering kernel for nuclei with pronounced resonances. The validation of this analytical approach is obtained by integrating the differential kernel over all spatial angles and energies of the scattered neutron. The obtained Doppler broadened scattering cross section is identical to the Doppler Broaden value given by the subroutine BROADR in NJOY [8].

In the current study these analytical differential and integral parts of the Doppler broadened cross section are confirmed by a modified stochastic algorithm. In particular, a subtle use of the basic Doppler broadening equation is presented, allowing for the generation of the Doppler broadened cross section in a straightforward manner. Consequently the three approaches [4], [5] and [9] are confirmed. The stochastic algorithm is applied to the Monte Carlo code MCNP as far as the scattering kernel is concerned. The method is compared to prepared S(α,β) scattering tables based on the analytical solution of the resonant dependent double differential scattering kernel of Rothenstein and Dagan [5, 6].

2. UNDERLYING SCHEME FOR STOCHASTIC DOPPLER BROADENING

The three analytical methods for Doppler broadening [4, 5, 9] presented above are subjected to the following expression of Doppler Broadening:

$$\mathrm{v}s_x(\mathrm{v},\mathrm{T})=\int\int \mathrm{v}_r s_x(E_r,0)P(\vec{\mathrm{V}},\mathrm{T})\mathrm{d}\vec{\mathrm{V}} \tag{1}$$

where v is the velocity of the neutron, v_r is the relative velocity between the neutron and target nuclei, $\sigma_x(v_r,0)$ is 0 K cross section and $P(\vec{\mathrm{V}},\mathrm{T})$ is the target nuclei velocity distribution. It is important to note that all three methods assume an ideal gas model using the Maxwell-Boltzmann distribution for the target nuclei agitation.

In the current study we adopt part of the “Sampled Velocity of the Target” (SVT) methodology within the COLLIDN subroutine of the MCNP code. Based on the probability density function $P(V,T)$ the speed of a target V nuclide is sampled [7]:

$$P(V,T)=\frac{4}{\sqrt{p}}b^3V^2e^{-b^2V^2},\quad b=\left(\frac{Am}{2k_BT}\right)^{1/2} \tag{2}$$

where k_B is the Boltzmann constant, Am is the mass of the target nuclide and T the temperature. The angle between the incident neutron and the sampled nuclei is chosen from an isotropic distribution. In order to associate a weight to the neutron interaction with the sampled target the relative neutron velocity is determined. The weight is then according to Eq. 1:

$$w_i=\frac{v_r}{v}s_x(v_r,0) \tag{3}$$

This sampling procedure is repeated N times. By accumulating all repetitive histories of those weighted probabilities at each energy point, one gets the Doppler broadened cross section:

$$s_x(\mathrm{v,T}) = \frac{1}{\mathrm{N}} \sum_{i=1}^{N} w_i \tag{4}$$

In addition, for scattering events the energy and the polar scattering angle of the emitted neutron are stored with the specific weight into energy and angular bins. The double differential part of the effective cross section, namely the scattering kernel, can therefore be evaluated by considering only a single energy and angular bin:

$$\frac{\partial s_s(\mathrm{v,T})}{\partial \mathrm{E} \partial \Omega} = \frac{1}{\mathrm{N}} \sum_{i=1}^{N} w_i^{bin} \tag{5}$$

2.1. The Stochastic Doppler Broadening of the Integrated Cross Section

A comparison between the stochastic Doppler broadening and the analytical method of the SIGMA1 approach within the NJOY processing code was performed for the total and scattering cross section of U238 at different temperatures using JEFF-3.1 nuclear data [10]. Figure 1 shows the Doppler broadened scattering cross section at 1200 K. Figure 2 shows the total cross section of U238 at 600 K. The energy scale ranges from 32 eV to 40 eV and covers the 3rd main S resonance of U238. Both figures show clearly that a stochastic procedure of Doppler broadening gives exactly the same Doppler broadened cross section in comparison with the analytical solution done in NJOY.

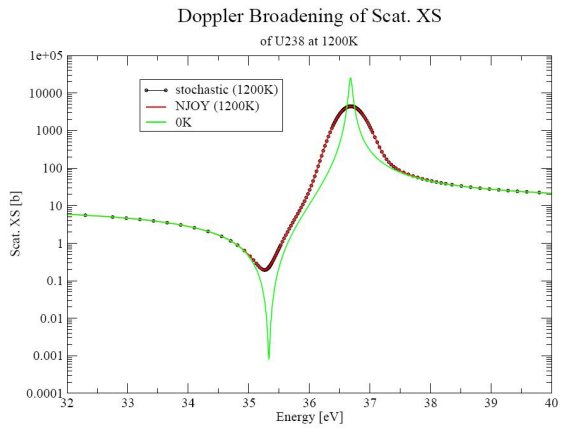

Figure 1: Doppler broadening of the scattering cross section of U238 at 1200 K by analytical and stochastic means and 0 K cross section

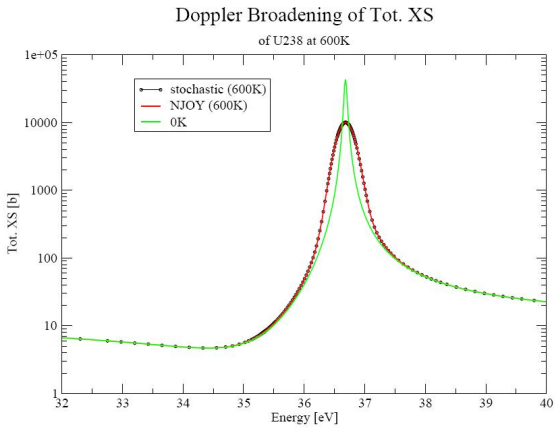

Figure 2: Doppler broadening of the total cross section of U238 at 600 K by analytical and stochastic means and 0 K cross section

2.2. The Stochastic Doppler Broadening of the Double Differential Scattering Kernel

The stochastic Doppler broadening method is used in this section to determine the differential part of the scattering cross section. This scattering kernel is very important as it appears explicitly in the transport equation. Especially in the vicinity of scattering resonances the reference kernel differs significantly from the commonly used asymptotic kernel for constant cross sections.
As mentioned above, the full double differential scattering cross section for heavy nuclei was presented in 1998 by Rothenstein and Dagan [5]. This free gas scattering kernel is given by integration over the initial and secondary velocities (*u* and *u'*) of the neutron in the target at rest frame, over the velocity of the center of mass (*c*), over the cosines of the polar angles of the incident and secondary neutrons (μ_u and $\mu_{u'}$) and over the cosine of the azimuth angle φ:

$$s_s^T\left(E\to E',\vec{\Omega}\to\vec{\Omega}'\right)=\frac{1}{2p}s_s^T\left(E\to E',m_0^{lab}\right)=$$
$$\frac{1}{2pv}\left(\frac{A+1}{A}\right)^4\left(\frac{A}{p}\right)^{3/2}$$
$$\int_0^\infty 2pu^2du\int_{-1}^{1}dm_u\int_0^\infty c^2dc\int_0^\infty (u')^2du'\int_{-1}^{1}dm_{u'}\int_{-1}^{1}\frac{2}{\sin j}d\cos j\,\frac{d\{u'-u\}}{(u')^2}\exp\left[v^2-(A+1)\left(\frac{u^2}{A}+c^2\right)\right]$$
$$\frac{1}{uvc}d\left\{m_u-\left[\frac{\left(v^2-c^2-u^2\right)}{2uc}\right]\right\}\frac{1}{2u'ck_BT}d\left\{m_{u'}-\frac{\left[(v')^2-(u')^2-c^2\right]}{2u'c}\right\} \qquad (6)$$
$$\frac{4vv'c^2}{B_0'}d\{\cos j-\cos\hat{j}\}\,us_s(E_r,0)\frac{P\left(u,m_0^{CM}\right)}{2p}$$

The variables μ_u, *u'*, $\mu_{u'}$ and *cos* φ are constrained by delta functions. In addition, the integrant contains the Maxwell-Boltzmann distribution of the target velocity, the scattering probability density in the center of mass frame $P(u, \mu_0^{CM})$ and the zero Kelvin scattering cross section $\sigma_s(E_r,0)$ evaluated at the energy of the incident neutron in the target at rest frame. For a full derivation of the kernel and extensive explication see [5].

We compare the resonant dependent stochastic kernel and the resonant dependent analytical kernel based on the solution given by Eq. 6. Figures 3 to 7 show different scattering kernel at different temperatures and at various energies. 10 million histories were sampled for the generation of the stochastic kernel. The scattering kernels give the probability that a neutron is scattered at a specific energy and in a specific spatial direction. The contour of the figures represents the energy distribution of the scattered neutron. Each segment of the kernel depicts a specific cosine direction bin i.e. the space is divided into 8 cosine equal segments.

Figures 3 to 6 show a comparison of the stochastic and analytical U238 kernel at different energies (6.53 eV, 21.5 eV, 35.3 eV) and different temperatures (300K, 600K, 1200K). 6.53 eV corresponds to the lower interference dip of the 6.67eV main S resonance of U238 while 21.5 eV

and 35.5 eV are at the lower and higher energy side of the 2nd and 3rd main S resonance. Figure 7 shows stochastic and analytical kernels for Th232 at 1200 K and 23.2 eV in the lower interference range of the 2nd main S resonance. The agreement of the stochastic and analytic kernel is good for all considered cases. The stochastic kernels exhibit small numerical instabilities for the forward scattering bin.

3. IMPLEMENTATION OF THE STOCHASTIC DOUBLE DIFFERENTIAL SCATTERING KERNEL INTO MCNP

As mentioned above the stochastic procedure to calculate the scattering kernel uses partly MCNP routines. Therefore MCNP is in principle able to determine the correct resonant dependent scattering kernel itself based on Doppler broadening. MCNP uses a probability density function for the target velocity and its direction μ_t in order to sample the targets for the neutron interaction [7]:

$$P(V,m_t)=\frac{v_r s_s(v_r,0)P(V,T)}{2v s_s(v,T)} \tag{7}$$

where *P(V,T)* is given by Eq. 2. Furthermore the MCNP code approximates:

$$\frac{s_s(v_r,0)}{s_s(v,T)}\approx 1 \tag{8}$$

This is only valid if the scattering cross section is constant.

In 1996 Rothenstein proposed to use an additional rejection method in MCNP. In [12, 13] it is shown that the probability density function can be written as:

$$P(V,m_t)=C'\left\{\frac{s_s(v_r,0)}{s_s^{\max}(v_x,0)}\right\}\left\{\frac{v_r}{v+V}\right\}\left\{\frac{(2b^4)V^3e^{-b^2V^2}+(bv\sqrt{p}/2)(4b^3/\sqrt{p})V^2e^{-b^2V^2}}{1+bv\sqrt{p}/2}\right\} \tag{9}$$

where:

$$C'=\frac{s_s^{\max}(v_x,0)(1+bv\sqrt{p}/2)}{s_s(v,T)vb\sqrt{p}} \tag{10}$$

The normalization constant C' depends on the neutron speed *v*, but neither on the speed *V* of the target, nor on the neutron speed v_r relative to the target at rest. The probability density function consist of three parts: the last factor is the density function from which the target velocity *V* is sampled. The first two factors in curly parenthesis represent two constraints on the chosen value

of V. The ratio $v_r / (v + V)$ cannot exceed unity and a rejection technique is applied in MCNP. The first term is expressed by the ratio of zero Kelvin scattering cross section in the target at rest frame and the maximum zero Kelvin scattering cross section. It is the part which MCNP neglects. In the modified MCNP version an additional rejection procedure, namely the Doppler Broadened Rejection Correction (**DBRC**), is introduced allowing for Doppler broadening of the scattering kernel. This scheme, albeit accurate, increases significantly the number of rejected sampling in the vicinity of resonances.

Basically this is a similar approach to the stochastic Doppler broadening in the previous section. But instead of using a weighting method a rejection procedure is applied. By consequence each scattering event based on an accepted sampled target has the weight one.

The DBRC method was implemented into the MCNPX Version 2.6 and MCNP5 source code. As the original scattering treatment in the relevant epithermal energy range is identical in MCNP5 and MCNPX we refer here to the corrections of the so called standard MCNP treatment (and not MCNPX). The new modifications are valid for both codes.

3.1. Comparison of the Stochastic Resonant Dependent Kernel and the Constant Cross Section Kernel

In the following, the Doppler broadening of the scattering kernels for various nuclei are shown (Figures 8 to 12). The figures show a comparison of the resonant dependent kernel and the constant cross section kernel.

Figures 8 and 9 show the scattering kernel of U238 at the peak of the 6.67 eV resonance and at its lower energy interference range (6.53 eV). One can see that the scattering kernel Doppler broadening is similar to the integrated cross section, namely decreases near the peak of the resonance (Figure 8) and increases around the dip of the resonance as a consequence of a positive temperature gradient.

Figures 10 and 11 show the Doppler broadening of the scattering kernels of Au179 and Hg199 at the resonance energies 23.2eV and 33.5eV, respectively. There is a relative good agreement of the resonant dependent and constant cross section kernels at low temperature (100 K). However, at higher temperatures similar differences can be noticed as for the kernel of U238 at resonance peak (Figure 8).

Figure 12 shows the resonant dependent scattering kernel of Th232 at 23.2eV which corresponds to the interference range of the 2nd resonance. The scattering kernel at this specific energy (23.2 eV) is limited to a much smaller energy range than the standard MCNP kernel. The up scattering fraction is larger for the DBRC model.

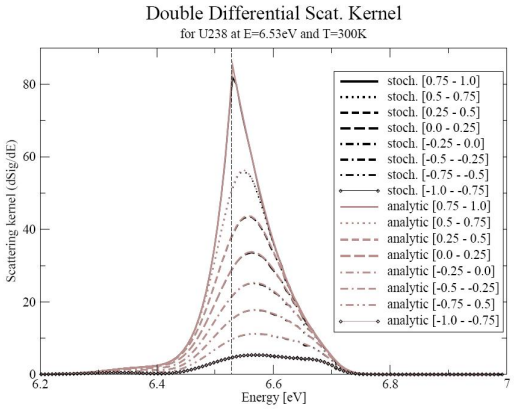

Figure 3: Stochastic and analytic resonant dependent scattering kernel of U238 at 6.53 eV and 300 K

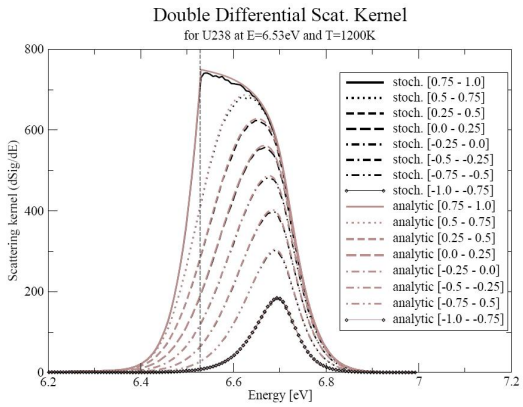

Figure 4: Stochastic and analytic resonant dependent scattering kernel of U238 at 6.53 eV and 1200 K

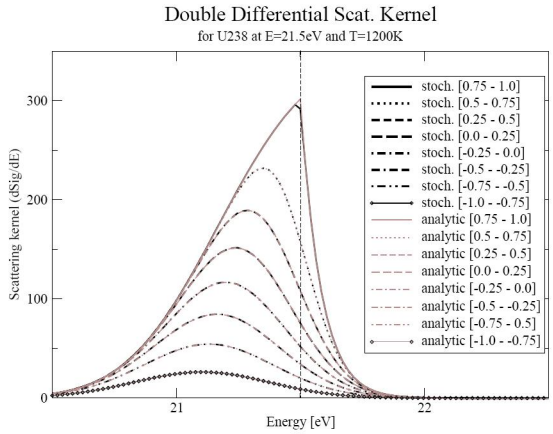

Figure 5: Stochastic and analytic resonant dependent scattering kernel of U238 at 21.5 eV and 1200 K

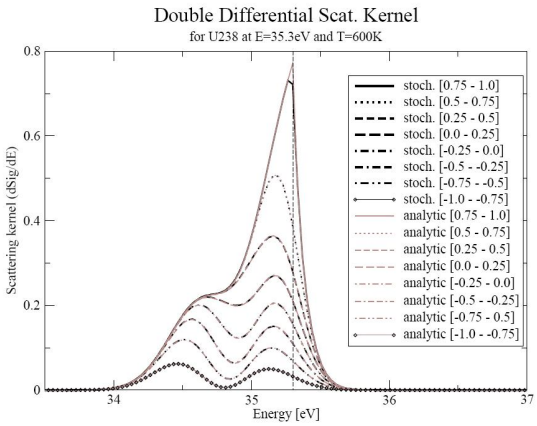

Figure 6: Stochastic and analytic resonant dependent scattering kernel of U238 at 35.3 eV and 600 K

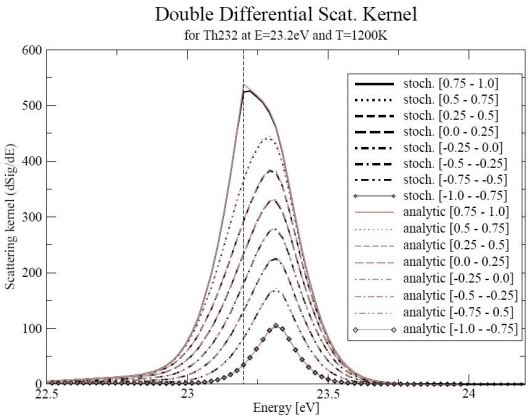

Figure 7: Stochastic and analytic resonant dependent scattering kernel of Th232 at 23.2 eV and 1200 K

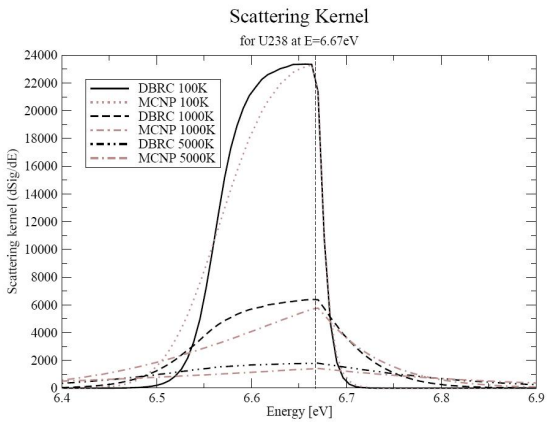

Figure 8: Stochastic resonant dependent kernel (DBRC) and constant XS kernel (MCNP) of U238 at 6.67 eV and for various temperatures

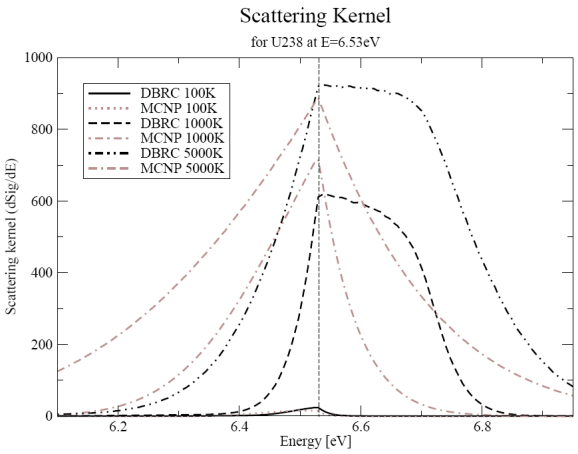

Figure 9: Stochastic resonant dependent kernel (DBRC) and constant XS kernel (MCNP) of U238 at 6.53 eV and for various temperatures

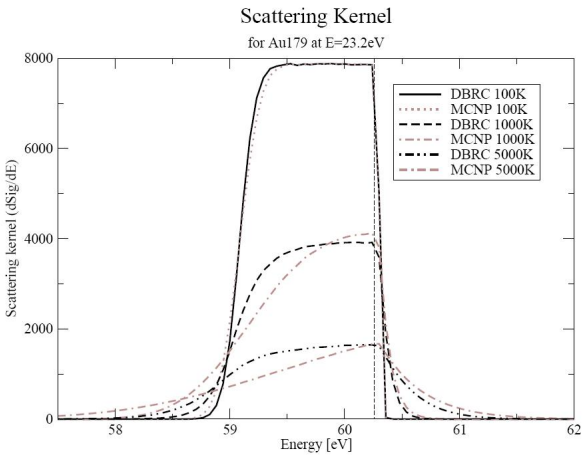

Figure 10: Stochastic resonant dependent kernel (DBRC) and constant XS kernel (MCNP) of Au197 at 23.2 eV and for various temperatures

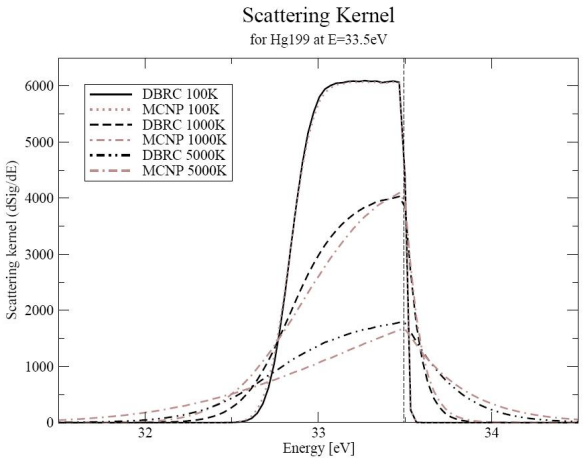

Figure 11: Stochastic resonant dependent kernel (DBRC) and constant XS kernel (MCNP) of Hg199 at 33.5 eV and for various temperatures

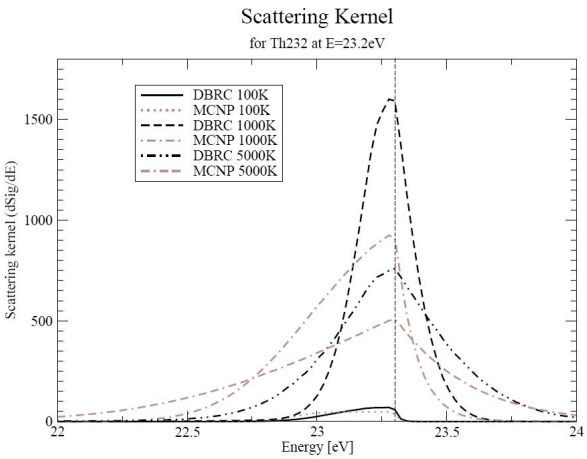

Figure 12: Stochastic resonant dependent kernel (DBRC) and constant XS kernel (MCNP) of Th232 at 23.2 eV and for various temperatures

It should be pointed out that the DBRC method as well as the existing S(α,β)-scattering tables approach remove the inconsistency between the integral and differential part of the Doppler broadened cross section and therefore should always be accounted for if the free gas model is applied. The validity of the free gas model is beyond the scope of this study. However we take notice of the scattering experiment of U238 performed by Danon et. al. at the Rensselaer Polytechnic Institute [16]. This experiment confirmed to a large extent the underlying model of the resonant dependent scattering kernel used by the DBRC and S(α,β)-scattering approach at 300K.

3.2. Comparison of Pin Cell Calculations for DBRC, the Analytic Resonant Dependent Kernel and the Standard MCNP Kernel

3.2.1. Criticality and reaction rates

The different scattering models are investigated for an infinite array of identical fuel pin cells. The pin model is based on a PWR subassembly benchmark proposed by Porsch et. al. [14]. UOX fuel elements are used with an enrichment of 4w/o U235. We compare four different scattering options applied for the U238 neutron scattering (Table I):

1. The standard MCNP scattering which uses the SVT subroutine for neutrons with energy up to $400k_BT$
2. The standard MCNP SVT model used for neutrons with energy up to 210eV
3. 1260 resonant dependent S(α,β) scattering tables with 16 polar scattering cosine bins and an energy range of 210eV. The S(α,β) were prepared with a modified version of the data processing code NJOY based on the analytical solution of the double differential resonant scattering kernel.
4. The new integrated stochastic DBRC option for neutrons with energy up to 210eV

The results of the pin cell study (Table I) show that the criticality calculation based on the DBRC model is in good agreement with the calculation based on S(α,β) tables. The difference is within the range of 20 pcm. Due to multiple rejections the computer time increases by about 20%.The criticality values in which the constant XS scattering models (Table I: 1, 2) were introduced are by far higher in comparison with the resonant dependent scattering models (Table I: 3, 4). The difference ranges from 340 to about 360 pcm.

In Table II capture reaction rates calculations are compared. The difference between the BDRC and S(α,β) tables based calculation is less than 0.3%. Contrarily the standard MCNP calculation differs significantly from both DBRC and S(α,β) tables algorithm by about 5.8% and 5.4% respectively.

Table I: Criticality k_∞ of a LWR pin cell at T_F=1200K and computer time (ctm) applying different scattering models

	Method	k_∞	ctm [min]
1.	standard MCNP: k_1	1.31137 +/-6E-5	1052
2.	standard MCNP (E_n<210eV): k_2	1.31153 +/-6E-5	1076
3.	S(α,β) : k_3	1.30772 +/-6E-5	1028
4.	DBRC: k_4	1.30791 +/-6E-5	1240
Differences	k_2-k_1	-16 pcm	
	k_3-k_1	-365 pcm	
	k_4-k_1	-346 pcm	
	k_4-k_3	19 pcm	

Table II: Capture reaction rate of a LWR pin cell at TF=1200K applying different scattering models

Energy bin [eV]	Capture reaction rate r [arb. Unit] (sdev. < 4E-6)			Differences (sdev. < 0.13%)		
	std. MCNP: r_1	S(α,β): r_2	DBRC: r_3	$(r_2-r_1)/r_1$	$(r_3-r_1)/r_1$	$(r_3-r_2)/r_2$
4.0 - 9.88	1.108E-02	1.110E-02	1.110E-02	0.22%	0.22%	0.00%
9.88 - 16.0	4.129E-04	4.119E-04	4.117E-04	-0.24%	-0.28%	-0.04%
16.0 - 27.7	6.173E-03	6.313E-03	6.311E-03	2.27%	2.24%	-0.03%
27.7 - 48.1	4.799E-03	5.079E-03	5.062E-03	5.84%	5.48%	-0.34%
48.1 - 75.5	2.328E-03	2.371E-03	2.370E-03	1.83%	1.81%	-0.02%
75.5 - 149	4.227E-03	4.262E-03	4.249E-03	0.83%	0.53%	-0.30%

3.2.2. Doppler reactivity benchmark

A comparison of the standard MCNP scattering model, S(α,β) scattering table based analytical model for resonant scattering of heavy nuclei (Eq. 6) and the DBRC stochastic model is done based on the Mosteller Doppler defect benchmark [11]. The benchmark consists of LWR fuel pin cells containing normal or enriched UO_2 fuel, reactor-recycle mixed-oxide (MOX) fuel or weapons-grade MOX fuel. The criticality of the pin cell is calculated for hot zero power (HZP) and hot full power (HFP). At HZP level all temperatures are assumed to be 600K. At HFP the fuel temperature increases to 900K. Further specifications are given in [11].

The Doppler coefficient of reactivity (DC) is calculated as:

$$DC = \frac{\Delta r_{Dop}}{\Delta T_{Fuel}} \tag{11}$$

where:

$$\Delta r_{Dop} = \frac{k_{HFP} - k_{HZP}}{k_{HFP} \cdot k_{HZP}} \tag{12}$$

The DC based on the different scattering models was calculated using JEFF3.1 data. The analytical approach with S(α,β) probability tables (16 cosine bins) and the DBRC model give equivalent results within 1 standard deviation for all three considered fuel types and independently of the fuel enrichment (Figures 13 to 15). A significant difference of 8 to 16% of the Doppler defect is found between the resonant dependent scattering kernels compared to the standard MCNP kernel. The Doppler coefficient is always increased applying the resonant dependent scattering models independently of fuel type and enrichment. Similar results for the UO_2 case were also obtained by [15].

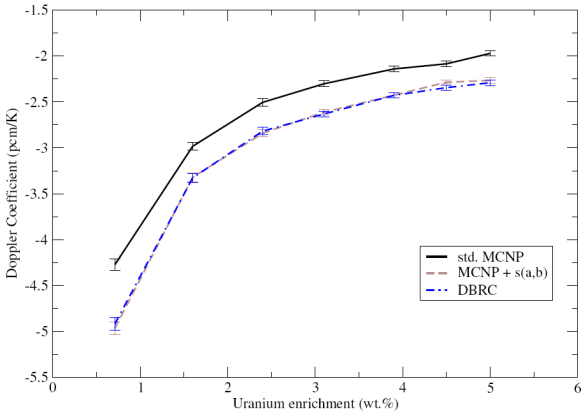

Figure 13: Doppler coefficient for UO_2 fuel based on different scattering models

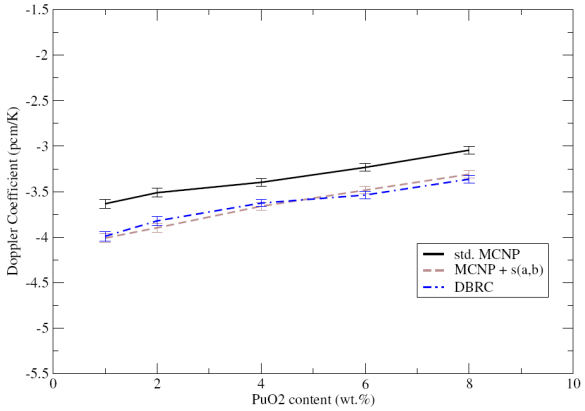

Figure 14: Doppler coefficient for reactor-recycle MOX fuel based on different scattering models

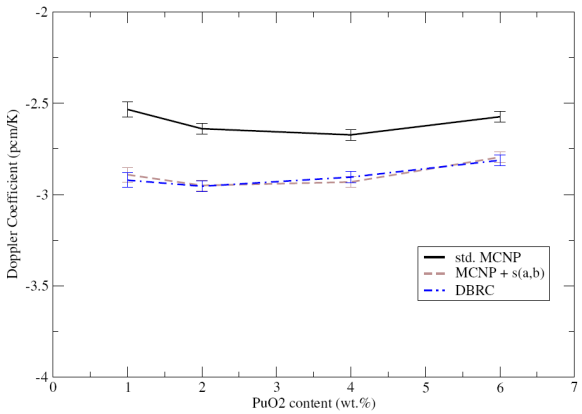

Figure 15: Doppler coefficient for weapons-grade MOX fuel based on different scattering models

4. CONCLUSIONS

The current study introduces an independent stochastic approach to calculate the Doppler broadened cross sections. It confirms for the first time the modified analytical resonant dependent scattering kernel for heavy isotopes with a complete different methodology. Both, the total (integrated) Doppler broadened cross section and its double differential part agree with the analytical solutions obtained by [4], [5] and [9]. The stochastic resonant dependent scattering kernel for heavy nuclei, namely the DBRC method, was integrated into MCNP.. For selected cases it is compared to the improved kernel introduction via S(α,β) scattering tables and to the standard MCNP model. It is shown that the new DBRC method gives the same results as the S(α,β) method within 1–2 standard deviations for all practical cases that were analyzed.

ACKNOWLEDGMENTS

The authors would like to acknowledge the support of EnBW Kernkraft GmbH.

REFERENCES

1. E. P. Wigner, E. J. Wilkins AECD-2275, Clinton Laboratory, (1944)
2. H. D. Brown and D. S. St. John, Oak–Ridge report DP-33, (1954)
3. G. L. Blackshaw and R. L. Murray, *Nucl. Sci. Eng.*, **Vol. 27**, pp. 520-532 (1967)
4. M. Ouisloumen and R. Sanchez, "A Model for Neutron Scattering Off Heavy Isotopes That Accounts for Thermal Agitation Effects", *Nucl. Sci. Eng.*, **Vol. 107**, pp. 189-200 (1991)
5. W. Rothenstein and R. Dagan, "Ideal gas scattering kernel for energy dependent cross-sections," *Ann. Nucl. Energy*, **Vol. 25**, pp. 209-222 (1998)
6. R. Dagan, "On the use of S(α,β) tables for nuclides with well pronounced resonances," *Ann. Nucl. Energy*, **Vol. 32**, pp. 367-377 (2005)
7. X-5 Monte Carlo Team, "MCNP-A General Monte Carlo N- Particle Transport Code, Version 5," LA-UR-03-1987 (2003)
8. R. E. Macfarlane, D. W. Muir, "The NJOY Nuclear Data Processing System, Version 91", LA-12740-M (1994)
9. D. E. Cullen and C. R. Weisbin, "Exact Doppler Broadening of Tabulated Cross Sections," *Nucl. Sci. Eng.*, **Vol. 60**, pp.199-229 (1976)
10. A. Koning, R. Forrest, M. Kellet, R. Mills, H. Henriksson, Y. Rugama (Edts.), "JEFF Report 21: The JEFF-3.1 Nuclear Data Library," OECD (2006)
11. R. D. Mosteller, "The Doppler-Defect Benchmark: Overview and Summary of Results", *M&C + SNA 2007*, Monterey, California, April 15-19, 2007
12. W. Rothenstein, "Neutron Scattering Kernels in Pronounced Resonances for Stochastic Doppler Effect Calculations", *Ann. Nucl. Energy*, **Vol. 23**, pp. 441-458 (1996)
13. B. Becker, R. Dagan, G. Lohnert, "Proof and implementation of the stochastic formula for ideal gas, energy dependent scattering kernel", *Ann. Nucl. Energy*, available online (2009)
14. D. Porsch, U. Hesse, W. Zwermann, W. Bernnat, AAA User-Group Workshop, Gesellschaft für Anlagen- und Reaktorsicherheit (GRS) mbH, Garching, Germany (2004)
15. Lee D., Smith K., Rhodes J., "The impact of 238U resonance elastic scattering approximations on thermal reactor Doppler reactivity", Physor'08 Conf., Sep. 14-19 (2008)
16. Y. Danon, R. C. Block, N. Francis, M. Lubert, M. Rapp, F. Saglime, R. Bahran, C. Romano, J. Thompson, D.P. Barry, N.J. Drindak, J.G Hoole, G. Leinweber, Molly Ernesti, "Cross Section Measurements and Analysis at Rensselaer", Report to CSEWG, November (2008)